JOURNAL OF APPLIED ELECTROCHEMISTRY **27** (1997) 1283–1289

Evaluation of anode deactivation in chlor-alkali cells

A. S. PILLA, E. O. COBO, M. M. E. DUARTE, D. R. SALINAS*

Instituto de Ingeniería Electroquímica y Corrosión, Departamento de Química e Ingeniería Química, Universidad Nacional del Sur, Av. Alem 1253, 8000 Bahía Blanca, Argentina

Received 20 December 1994; revised 24 February 1997

Different techniques to evaluate catalytic activity and to quantify residual service life (RSL) have been applied to DSA® anodes used in chlor-alkali industrial cells. An accelerated service life test in sulfuric acid was used as a reference method. The results obtained through EIS, cyclic voltammetry and Ru content analysis of the catalytic layer confirm the results obtained with the accelerated test. There is a direct relation between the residual service life (RSL) thus obtained and the catalytic properties of the electrode. The different mechanisms of catalytic activity loss are discussed. An evaluation methodology is proposed to reduce maintenance costs of industrial cells.

Keywords: *Chlor-alkali cells, dimensionally stable anodes*

1. Introduction

Dimensionally stable anodes (DSA®) are widely used in the chlor-alkali industry because of their durability and low chlorine overvoltage. During operation, the electrode catalytic coating suffers a progressive degradation which is manifested by an increase in the cell operating potential. This is usually the only operating parameter that indicates loss of anode catalytic activity. As the total anodic surface area of a cell comprises that of many individual anode plates, it is difficult to localize damaged units. Moreover, local differences in the anode properties are more noticeable in mercury cells where short circuits between anode and cathode are a frequent problem. Therefore, the usual, but costly, solution is to recoat the whole anode assembly.

The evaluation of the anodes state is not practical using industrial operating conditions because of the long time it involves. Several tests have been developed to obtain a quick evaluation of the service life and/or the stability of these DSA®-type electrodes [1–10]. Most of these can be classified as accelerated life tests. They are based on the application of a constant current with simultaneous recording of potential change with time. The electrode behaviour is found to be dependent on the nature of the electrolytic medium. Sulfuric acid [1, 2, 10], dilute sodium chloride [9] and sodium hydroxide [8] solutions are the electrolytes most frequently used in the experiments. Other techniques such as a.c. impedance spectroscopy [5, 6] and cyclic voltammetry [7, 10] have also been suggested.

The results obtained in the works described above are difficult to compare quantitatively because electrodes with variable catalytic coating molar ratios of RuO_2/TiO_2 were prepared using different methods.

The aim of this work is to analyse results obtained by several of the above mentioned techniques and to define a simple and reliable routine procedure for the residual service life (RSL) evaluation of industrial DSA® electrodes.

2. Experimental details

Samples obtained from 'spaghetti'-type DSA® industrial electrodes employed in chlor-alkali mercury cells were used for the experiments. The samples were cylinders ($\phi = 0.3$ cm) of 1 cm^2 geometrical area with nominal operation times ranging from 0 to 36 months.

Accelerated life tests were carried out in 2 M H_2SO_4 solution using a conventional glass cell. A constant current was applied to the sample and the potential variation with time was recorded [1, 2]. The counter electrode was a platinized platinum foil and the reference was a saturated calomel electrode placed near the anode through a Luggin capillary. The electrolyte was circulated to maintain a constant temperature ($T = 25\,°C$) and to avoid accumulation of electrolysis products. A Wenking HP88 potentiostat was used to apply a constant voltage to a fixed resistance in series with the cell, giving a constant current through the circuit. An X–t recorder was used to follow the potential variation. All potential values in the text were referred to the standard hydrogen electrode.

The ruthenium content in the catalytic layer was measured by dissolving the samples coating in a fused mixture of NaOH and $NaNO_3$ [11] at 450 °C. The residue was digested in water and the resulting solution was acidified with HCl. The ruthenium concentration was determined by atomic absorption spectroscopy.

Changes in coating morphology and thickness were followed by optical and electronic scanning

* To whom correspondence should be addressed.

microscopy. An Olympus PME metallurgical microscope and a Jeol 100 scanning electronic microscope were used. For lateral surface studies, small fragments of the electrodes were mounted on copper supports and plated with gold. Samples for transverse view observations were embedded in epoxy resin and polished to mirror finish. Coating thickness was measured by optical microscopy and reported here as the average of twenty values taken around the electrode contour.

Cyclic voltammetry was carried out in a conventional glass cell using continuous sweeps in the potential range $0.05\,V \leq E \leq 1.25\,V$. The sweep rate was $0.05\ V\ s^{-1}$ and the electrolyte was $0.5\,M\ H_2SO_4$ solution. Steady-state voltammograms were recorded while the anodic sweep charges were measured using a digital coulometer.

Impedance measurements were performed in $0.5\,M\ H_2SO_4$ solution at $E = 1.5\,V$, using oxygen evolution as test reaction. Measurements were carried out applying a small amplitude sine wave voltage (10 mV peak-to-peak), with a Solartron FRA 1172 frequency analyser, jointly with a Solartron 1286 electrochemical interface commanded by a HP 9000 computer. The frequency range was 65.5 kHz–0.002 Hz.

3. Results and discussion

3.1. *Accelerated life test*

In the accelerated life test one variable (potential or current) is fixed and the other is recorded during the test. Anode deactivation is indicated when current falls (constant potential) or when potential rises steeply (constant current). A typical response for the latter is shown in Fig. 1 in which an extended zone with slight potential variation is observed, followed by a swift rise to higher potential. The time for the voltage to rise to 10 V defines the failure time (FT). This value is the time required for total removal of the electroactive surface layer [3] and can be used as a relative measure of the RSL for a given electrode. Figure 1 shows that *FT*, defined in this work as the intersection of the tangents to the curve, can also be quantified in different forms. *FT* values show similar trends although they depend on the experimental procedure.

Two accelerated life tests records are shown in Fig. 2. Whereas samples obtained from an unused electrode show an *FT* close to 16 h for a current density of $1.5\,A\,cm^{-2}$, totally deactivated samples fail after a few minutes.

The current distribution and the electrolyte composition are important factors affecting the *FT* results [1, 2, 9]. The *FT* is also strongly dependent on current density. For example, when current density increases from $1.5\,A\,cm^{-2}$ to $2\,A\,cm^{-2}$, the *FT* value falls to half of its original value.

Operation times reported in industry are based on continuous operation of a given cell. Samples obtained from various locations in a mercury cell show significant differences in the state of their catalytic coating owing to local differences in current distribution and short circuits between anode and cathode. Therefore, *FT* values of samples obtained from different electrodes of the same cell vary and it is impossible to find an exact and quantitative relation between cell operation time and electrode failure time. Nevertheless, for individual samples the failure time, determined for the accelerated life test, may be used as an indication of their residual service life. Although the accelerated life test is confined to samples that are a small part of an anode (size = $0.6\,m \times 0.6\,m$), its catalytic state may be evaluated by taking several samples from it and performing the accelerated life test to obtain the FT_i values. This strategy requires an appropriate sample collection: the current distribution should not be changed too much and the location of the samples should represent the total anode state.

Hence, it is necessary to determine if the failure time thus obtained relates to the sample catalytic

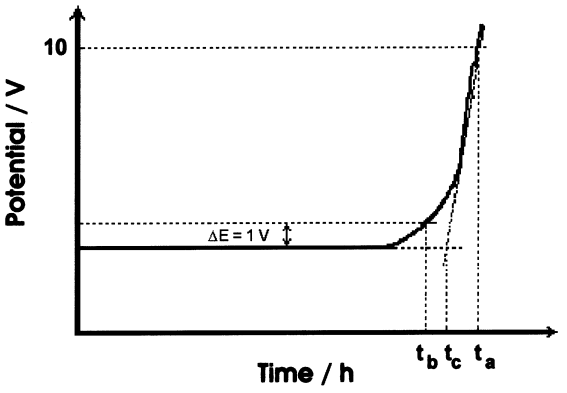

Fig. 1. Determination of failure time in $2\,M\ H_2SO_4$ at $1.5\,A\,cm^{-2}$. t_a: time when the sample potential reaches 10 V; t_b: time when the sample potential reaches 1 V with reference to the initial potential; t_c: time obtained from the intersection of the tangents to the curve.

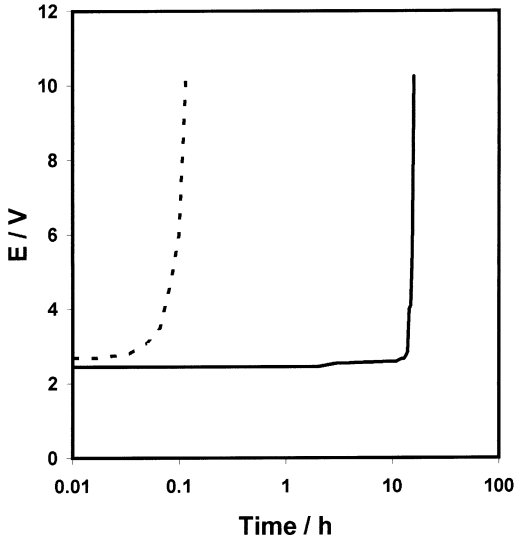

Fig. 2. Potential variation with time for electrodes with different catalytic states throughout the accelerated life test in $2\,M\ H_2SO_4$ ($i = 1.5\,A\,cm^{-2}$). Key: (——) unused electrode; (- - - -) deactivated electrode.

conditions. In the following discussion, the catalytic state of different samples is evaluated using different techniques and is compared to the corresponding *FT*. The possible deactivation mechanism involved is also analysed.

3.2. *Ruthenium content and microscopy studies*

The potential rise observed at the end of the accelerated life tests may arise from one of the following causes:

(i) Anodic oxidation of RuO_2 with formation of soluble Ru species [9].
(ii) Electrode active mass decrease through loosening of poorly adherent pieces of coating. This process is produced by the mechanical action of bubbles evolving in the coating cracks [11], or by mechanical erosion due to turbulent hydrodynamic conditions.
(iii) Substrate oxidation leading to electrical insulation of the coating. A nonconductive layer of Ti oxides formed at the interface between metal and the RuO_2–TiO_2 catalytic layer may be responsible for this behaviour [1, 2].

The remaining Ru content measurement per geometric area of electrode should give information about the coating state if mechanisms (i) or (ii) have operated. Table 1 shows a direct relation between the ruthenium content and *FT* for different samples. These results confirm that the coating degradation occurs along with the loss of catalyst.

In addition, samples with different *FT* show changes in the catalytic coating morphology. These results are consistent with a type (ii) deactivation mechanism. The surface of an unused electrode (Fig. 3(a)) shows the typical grooves and cracks of the catalytic coating produced by the manufacturing method. In the event of a partially deactivated electrode, the surface presents a more noticeable cracking (Fig. 3(b)). In totally deactivated electrodes, wide areas free of catalytic coating are observed (Fig. 3(c)). In some cases, big pieces of coating loosening from the electrode surface can be seen.

The electrodes evaluated with the accelerated life test in sulfuric acid solution (Fig. 3(d)) show morphological features similar to the electrodes degraded in industrial conditions (Fig. 3(c)). This observation indicates that the same deactivation mechanism operates in both cases.

The loss of electrode active mass can also be observed by measuring coating thickness of samples with different *FT*. Figure 4 shows transverse views of an unused electrode with the typical variations in the coating thickness as was demonstrated by Nidola [12]. Samples of these unused electrodes partially deactivated using the accelerated life test in sulfuric acid show a reduction in the coating thickness (Fig. 5). Likewise, the same phenomenon is observed in samples obtained from industrial mercury cells and the thickness of the remaining coating is directly related to the respective *FT* recorded (Fig. 6). The dispersion observed in the results appears because the anode coating is nonuniform in thickness, as can be seen in Figs 4 and 5.

Ru content measurements and microscopy studies indicate that DSA®-type electrode deactivation is produced, initially by a gradual loss of TiO_2–RuO_2

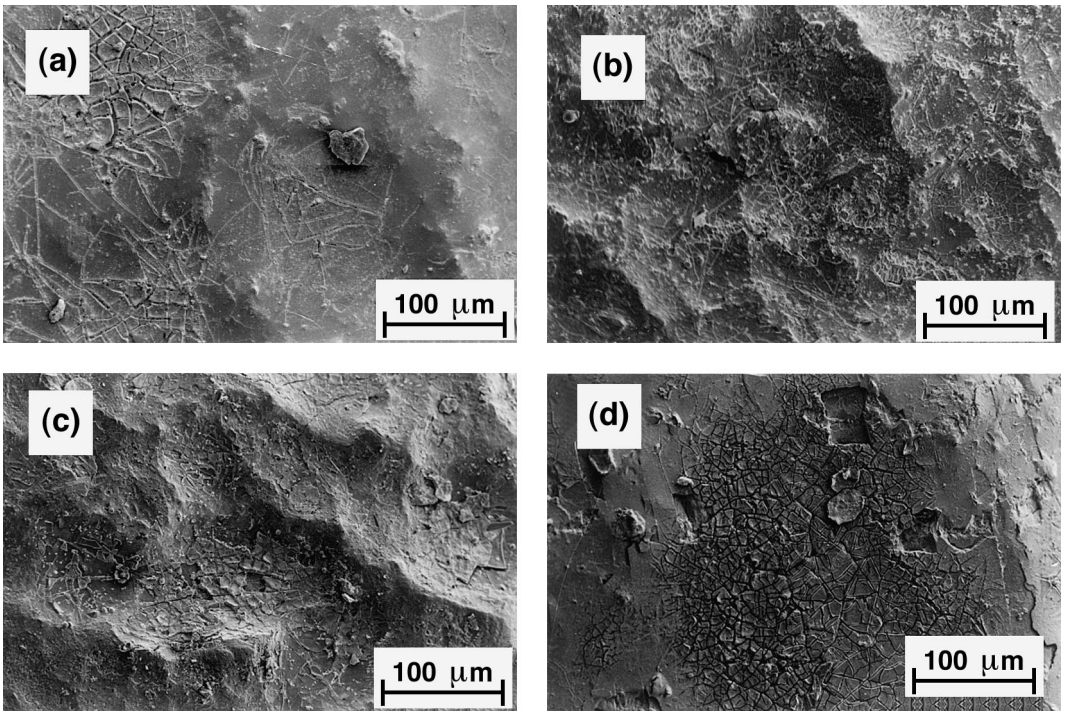

Fig. 3. SEM micrograph of the samples surface with different deactivation states. (a) Sample from an unused electrode (*FT* = 16 h); (b) partially deactivated sample (*FT* = 4.5 h); (c) totally deactivated sample (*FT* = 5 min); (d) sample from an unused electrode partially deactivated using the sulfuric acid test for 5 h.

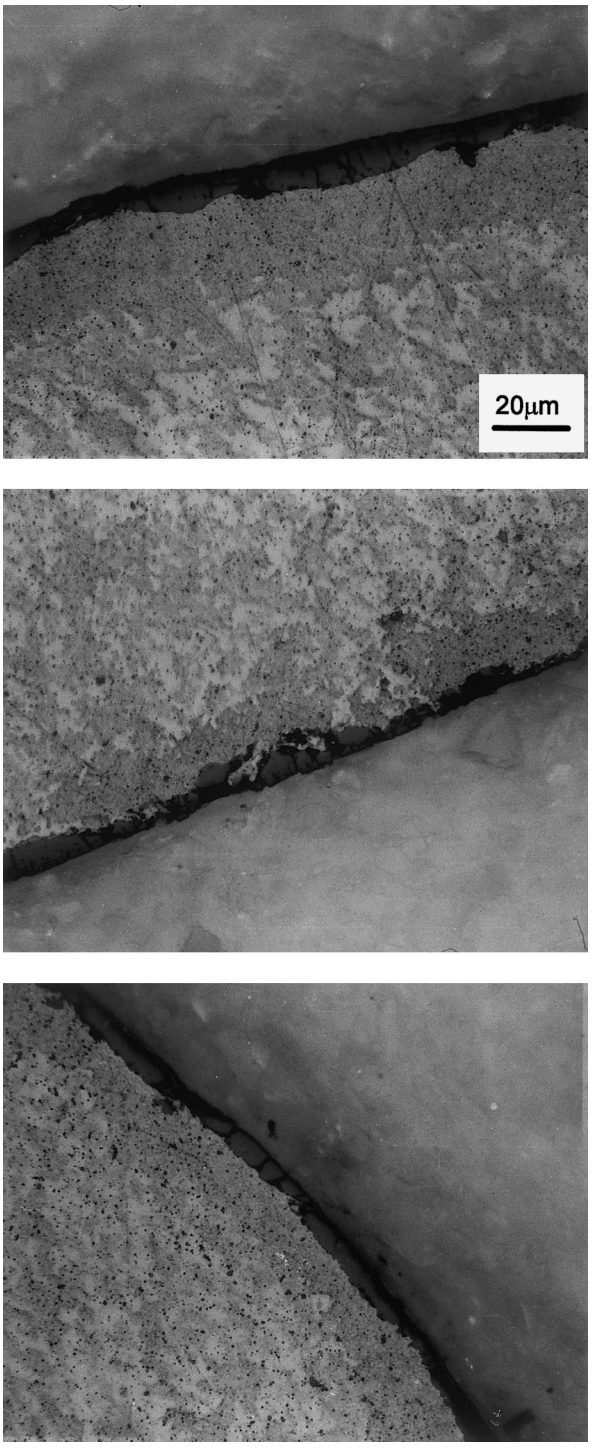

Fig. 4. Transverse views of an unused electrode showing the irregular thickness of the catalytic coating.

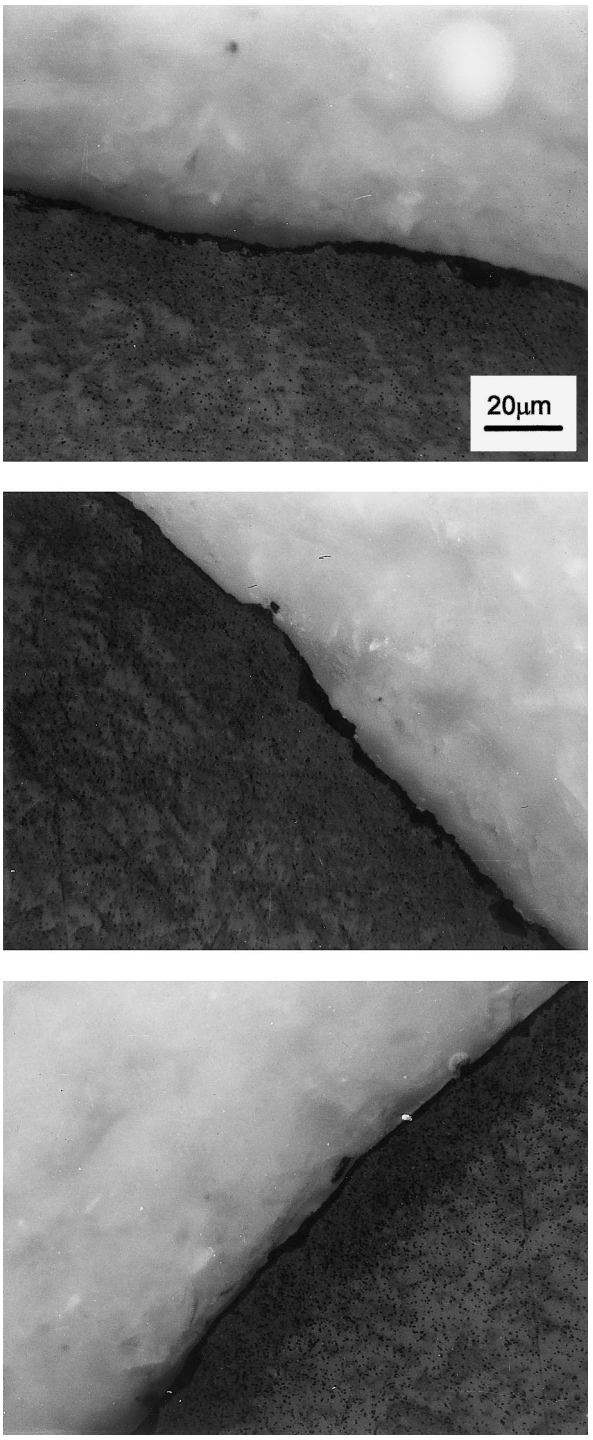

Fig. 5. Transverse views of an unused electrode after a partial deactivation in 2 M H_2SO_4 solution. $i = 1.5\,A\,cm^{-2}$.

coating. This coating loss is caused by dissolution and mechanical erosion processes. In later stages, coating pieces become less adherent and consequently, they detach from the electrode surface and fall into the solution. The same mechanism occurs in both sulfuric acid solutions and chloride solutions, but with differences in the rates involved. This fact is in agreement with Loucka [1] who proposed that the electrochemical activity loss is related to oxygen evolution. In chloride solutions the oxygen discharge rate is much slower than in sulfuric acid solutions. Accordingly, the time required to degrade the electrodes is very short in the second case. The phenomenon may be accentuated by bubbles evolving in the coating cracks. These bubbles produce mechanical tensions decreasing the catalytic coating adherence.

3.3. *Cyclic voltammetry*

This technique has been applied to DSA® to characterize electrode surface state [11, 13–18], determine oxide mixture compositions [7] and obtain a relative measurement of the real surface area [11, 19]. This technique has been suggested using the coulombic

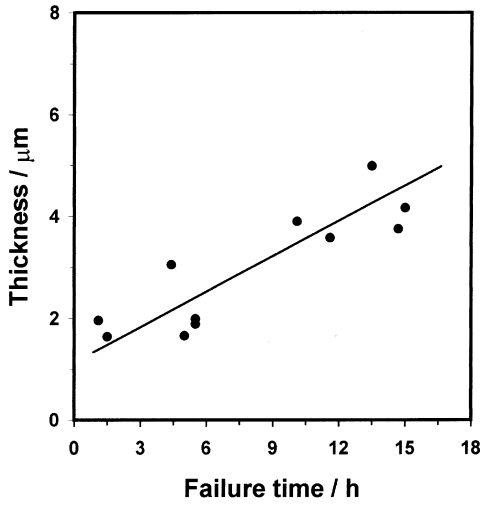

Fig. 6. Relation between the mean coating thickness and the respective *FT* of samples obtained from industrial electrodes.

charge transferred in the anodic half cycle (Q_a) to monitor the surface properties of oxide electrodes [3, 8]. The Q_a value depends on the potential range analysed, the sweep rate, and the electrolyte nature. The influence of these factors makes it necessary to standardize the measurement conditions to compare results from different electrodes.

Voltammograms of samples with different deactivation stages obtained in sulfuric acid solutions are shown in Fig. 7. For unused electrodes large background currents are observed (sample A). During the voltammetric experiment, the surface is oxidized and reduced reversibly through a mechanism involving proton exchange with the solution [20, 21]. The voltammetric charge is believed to be a measure of the number of sites able to exchange protons with the solution [22]. Thus, this voltammetric charge is a measure of the electrochemical real surface area [23]. The voltammogram of a sample extracted from an electrode used for 21 months in a mercury cell (sample B) is quite similar to one obtained with unused electrodes. However, higher current densities are observed. This effect may arise from an increase in roughness, which leads to a higher active surface area. These results are in agreement with those from microscopic examinations since the coating surface of this electrode and others with similar histories show a higher degree of cracking (Fig. 3(b)). The voltammogram is quite different in a completely deactivated sample (sample C). The current densities are lower than in the previous cases. At potentials close to zero there is an increase in the cathodic current density promoted by the beginning of the hydrogen reaction. Similar voltammograms are obtained with pure titanium electrodes which indicate a change in the chemical nature of the sample interface. This is in agreement with electron microscopy observations that show a nearly total catalytic coating loss in these samples.

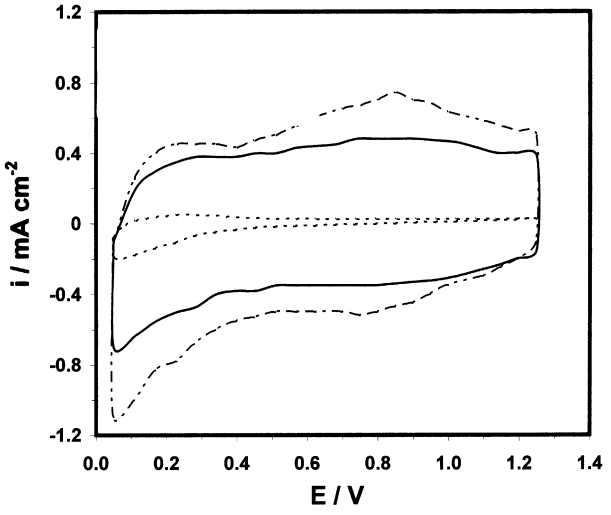

Fig. 7. Voltammograms of samples with different electrochemical activity: A: unused electrode; B: partially deactivated electrode in industrial conditions (*FT* = 10.5 h); C: totally deactivated electrode (*FT* = 5 min). Solution: 0.5 M H_2SO_4, $|dE/dt| = 0.05\,V\,s^{-1}$. Key: (——) sample A; (—··—) sample B; (- - - -) sample C.

Samples with different deactivation stages obtained from industrial cells were studied using both techniques to obtain the relation between Q_A and the *FT*. An increase in Q_A is observed while the sample *FT* decreases (Fig. 8). Only samples having a voltammetric response like samples A or B in Fig. 7 were included in Fig. 8. Samples with voltammograms like sample C were discarded because in those cases the total coating was lost, the Q_A recorded values were very low and the respective failure times were only a few minutes. Comparing Figs 6, 8 and Table 1 it is possible to conclude that, as the samples have lower *FT*, they show loss of Ru content and a coating thickness reduction together with a surface roughening. In addition, the relation between the *FT* and these parameters seems to be linear.

3.4. *Electrochemical impedance spectroscopy*

Studies using electrochemical impedance spectroscopy (EIS) [5] suggest that this technique is a sensitive tool to characterize the catalytic state of DSA®-type electrodes. In our work samples with different *FT* were tested with EIS using oxygen evolution as test

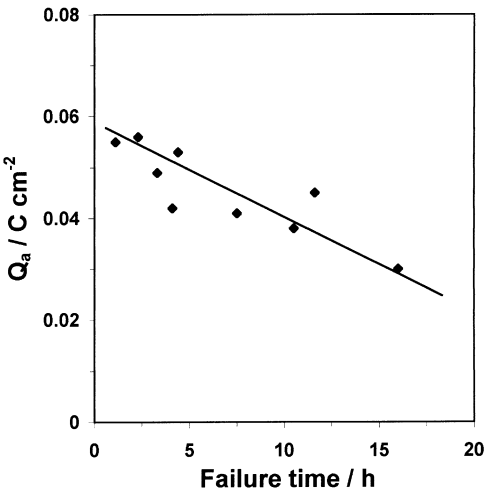

Fig. 8. Relation between the voltammetric anodic charge Q_a and the respective FT of the samples.

Table 1. Ruthenium content of electrodes with different deactivation stages and the corresponding FT

Sample	*Failure Time*/h	*Ru content*/mg cm^{-2}
A	16.0	2.00
B	14.7	1.80
C	13.5	1.70
D	10.1	1.00
E	8.6	0.85
F	7.5	0.60
G	5.5	0.39
H	2.5	0.13

reaction. Some of the impedance diagrams obtained in the complex plane are shown in Fig. 9. When the catalytic coating is still present, the diagrams are almost a perfect semicircle. This behaviour can be simulated by a transfer function corresponding to a simple equivalent circuit composed by the electrical double layer capacitance C_{dl} in parallel with the transfer resistance R_t, and this parallel RC circuit in series with the uncompensated electrolyte resistance R_{ohm} [24]. As the *FT* of the samples decreases, the diagrams show a slight reduction in the transfer resistance R_t. When the sample has practically no coating, which is corroborated by the voltammetric record and by measuring the coating thickness and Ru content, the *FT* is close to zero and the tendency in the impedance diagram changes. Thus, a very high increase in R_t and two time constants are observed (Fig. 9). Figure 10 shows the relation between the *FT* of the samples and the respective values of R_t and double layer capacity C_{dl} calculated from the time constant ($C_{dl} \times R_t$) [25]. In both (a) and (b) of Fig. 10 the tendencies of R_t and C_{dl} are indicated with dashed lines when no coating exists on the sample. The most important result from impedance measurements is that the double layer capacitance shows a nearly linear relation with the *FT*. Comparing Figs 8 and 10, it can be seen that the trend is similar to that observed for the anodic charge, although the dispersion degree

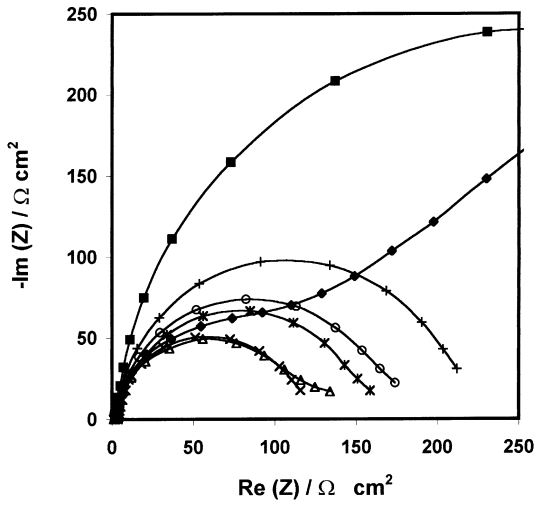

Fig. 9. Nyquist plot of samples with different *FT*. Solution: 0.5 M H_2SO_4; E = 1.5 V; amplitude 10 mV. *FT*: (◆) 0 min, (■) 5 min, (Δ) 1.5 h, (×) 3.3 h, (*) 7.5 h, (○) 10.5 h and (|) 16.2 h.

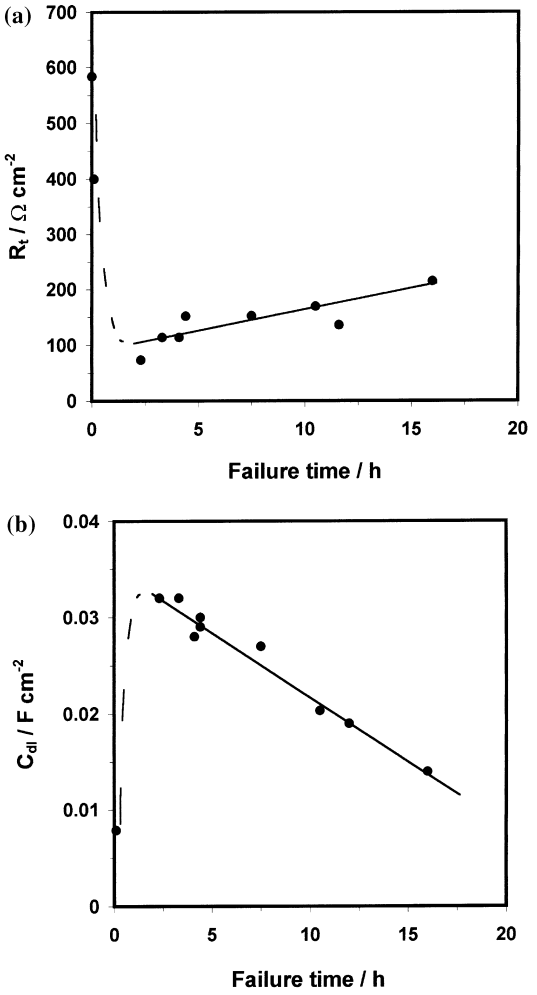

Fig. 10. Relation between the *FT* of the sample and (a) the charge transfer resistance R_t, (b) the corresponding double layer capacity C_{dl}.

is lower. An increase in surface roughness is probably the predominant contribution in the linear region of the curve. When the electrode has lost the catalytic layer, the capacity decreases drastically and falls to much lower values. The problem is to distinguish if an electrode with a relatively low capacity is a new electrode or a very worn out one. Looking at Figs 9 and 10 it can be seen that the R_t of most electrodes, ranges from 100 Ω cm^{-2} to 200 Ω cm^{-2}. In a completely deactivated electrode (e.g., FT = 5 min) the diagram shape changes, a second time constant appears and R_t is greater. On the other hand, cyclic voltammetry also show substantial changes in the records obtained for all these cases. Thus, by examining the response in voltammetric experiences, the impedance diagrams shape and the R_t values obtained, it is possible to deduce whether the sample has the features of a relatively unused electrode or the typical response of a deactivated one.

4. Recommended practice for RSL evaluation

Regardless of which deactivation mechanism takes places during the operation, a gradual loss of catalytic material with an increase in the surface rough-

ening is observed in DSA®-type electrodes. This conclusion was reached through microscopic studies as well as voltammetric and EIS measurements. It has been demonstrated that these effects are directly related with the failure time obtained with the accelerated life test in sulfuric acid solution. When the electrodes present greater deterioration, which is corroborated by thickness measurements and the ruthenium content analysis of the catalytic coating, failure times are shorter. This parameter has an adequate sensitivity and, consequently, its measurement constitutes a practical technique to determine the residual service life of industrial DSA®-type electrodes. On the other hand, *FT* shows a linear relationship with Q_A, R_t and the coating thickness. All these parameters could provide the necessary information to evaluate the anode catalytic state. From a practical point of view, the accelerated test in sulfuric acid and the cyclic voltammetry, are the easiest techniques to use in an industrial plant.

Taking into account the results obtained, we proposed the following method for evaluation of DSA® anodes in chlor-alkali cells:

(i) Cyclic voltammetry and the accelerated life test in sulfuric acid solution should be applied to samples of unused anodes to obtain the Q_A and FT_o values. The FT_o obtained corresponds to the residual service life (RSL_o) indicated by the manufacturer (five years in most cases). As the sample area is small compared with the total anode area, the choice of an adequate sampling policy is of utmost importance. Extraction sites should be chosen so as to obtain information about the total anodic area without altering current distribution conditions excessively.

(ii) Both techniques should be also applied to samples of used anodes to obtain the FT_i and Q_A values prior to deciding the anode recoating. The voltammetric response and the Q_A and FT_i values are compared with those obtained from unused anodes of the same lot.

(iii) Considering the FT_o, the RSL_o and the FT_i for the actual electrode, the RSL_i can be calculated by

$$RSL_i = \left(\frac{FT_i}{FT_o}\right) RSL_o$$

(iv) The voltammetric response and the Q_A value are used to verify that a catalytic layer is still present on the considered electrode.

(v) When EIS or microscopy techniques are available, they can be used to corroborate the results.

(vi) The *RSL* of the anode will be obtained by averaging the corresponding RSL_i values.

(vii) Anodes with similar *RSL* are reassembled , so as to operate with equivalent catalytic power in all of them.

(viii) Anodes with low *RSL* are sent to be recoated.

Implementation of an analysis programme, similar to that one indicated above, permits the development of a data base which will allow to a better knowledge of cell operation. This will also reduce cell maintenance costs since the recoating is carried out on the anodes that really need it and not on those which still show significant catalytic activity.

Acknowledgements

The authors thank Dr Jorge B. Bessone for helpful discussions and advice. The financial support of this work by the Universidad Nacional del Sur and INDUCLOR S.A. is gratefully acknowledged. M.M.E.D. acknowledges financial support from the Comisión de Investigaciones Científicas de la Provincia de Buenos Aires and E.O.C. also thanks the fellowship granted by the Consejo Nacional de Investigaciones Científicas y Técnicas.

References

[1] T. Loucka, *J. Appl. Electrochem.* **7** (1977) 211.
[2] *Idem., ibid.* **11** (1981) 143.
[3] L. D. Burke, M. E. Lyons and M. McCarthy 'Hydrogen as an Energy Carrier' (edited by G. Imarisio and As. Strub), D. Reidel (1983), p. 128.
[4] C. Iwakura, M. Inai, T. Uemura and H. Tamura, *Electrochim. Acta* **26** (1981) 579.
[5] J. A. Harrison, D. L. Caldwell and R. E. White, *ibid.* **29** (1984) 203.
[6] P. Narayanan Kutty, B. K. Sadananda Rao, R. D. Angal, *Bull. Electrochem.* **6** (1990) 217.
[7] C. Angelinetta, S. Trasatti, Lj. D. Atanasoska and R. T. Atanasoski, *J. Electroanal. Chem.* **214** (1986) 535.
[8] L. D. Burke, M. E. Lyons and M. McCarthy, Proceedings of the 4th World Hydrogen Energy Conference, Pergamon Press (1982), p. 267.
[9] F. Hine, M. Yasuda, T. Noda, T. Yoshida and J. Okuda, *J. Electrochem. Soc.* **126** (1979) 1439.
[10] Ch. Comninellis and G. P. Vercesi, *J. Appl. Electrochem.* **21** (1991) 335.
[11] D. M. Novak, B. V. Tilak and B. E. Conway, Fundamental and Applied Aspects of Anodic Chlorine Production *in* 'Modern Aspects of Electrochemistry', vol. 14 (edited by J. O' M. Bockris, B. E. Conway and R. White), Plenum Press (1982), chapter 4, p. 195.
[12] A. Nidola, Technological Impact of Metallico Oxides as Anodes, *in* 'Electrodes of Conductive Metallic Oxides' (edited by S. Trasatti), Elsevier Scientific (1980), part B, chapter 11, p. 627.
[13] R. S. Yeo, J. Orehotsky, W. Visscher and S. Srinivasan, *J. Electrochem. Soc.* **128** (1981) 1900.
[14] D. Galizzioli, F. Tantardini and S. Trasatti, *J. Appl. Electrochem.* **4** (1974) 57.
[15] M. Vukovic, *Electrochim. Acta* **34** (1989) 287.
[16] S. Ardizzone, G. Fregonara, S. Trasatti, *ibid.* **35** (1990) 263.
[17] T. A. Lassali, J. F. C. Boodts, S. C. de Castro, R. Landers and S. Trasatti, *ibid.* **39** (1994) 95.
[18] O. R. Camara and S. Trasatti, *ibid.* **41** (1996) 419.
[19] R. F. Savinell, R. L. Zeller and J. A. Adams, *J. Electrochem. Soc.* **137** (1990) 489.
[20] S. Trasatti and G, Buzzanca, *J. Electroanal. Chem.* **29** (1971) 1.
[21] K. Doblhofer, M. Metikos, Z. Ogumi and H. Gerischer, *Ber. Bunsenges. Phys. Chem.* **82** (1978) 1046.
[22] G. Lodi, E. Sivieri, A. De Battisti and S. Trasatti, *J. Appl. Electrochem.* **8** (1978) 135.
[23] L. D. Burke and O. J. Murphy, *J. Electroanal. Chem.* **96** (1979) 19.
[24] A. J. Bard and L. R. Faulkner, 'Electrochemical Methods. Fundamentals and Applications', Wiley (1980), p. 323.
[25] M. Sluyters-Rehbach and J. H. Sluyters, 'Electroanalytical Chemistry', vol. 4 (edited by A. J. Bard), Dekker (1970), p. 1.